Journal of Nanopores Systems

Original Research Paper

Molecular Dynamics Simulation of Favipiravir Adsorption Behavior on Natural Zeolites

Motahareh Noormohammadbeigi[1,2]

[1]*Department of Chemistry, Payame Noor University (PNU), Tehran, Iran;*
[2]*Department of Chemistry, Faculty of Science, Arak University, Arak 38156-8-8349, Iran.*

Article history
Received: 16 August 2024
Revised: 26 April 2025
Accepted: 2 May 2025

*Corresponding Author: Motahareh Noormohammadbeigi, Department of Chemistry, Payame Noor University (PNU), Tehran, Iran; Department of Chemistry, Faculty of Science, Arak University, Arak 38156-8-8349, Iran;
Email: Motahareh.beigi@yahoo.com.

Abstract: In this study, molecular dynamics simulation has been applied to investigate Heulandite family zeolites (Heulandite and Clinoptilolite differing in Si/Al content) adsorption capacity of Favipiravir acting as both a potential treatment candidate for COVID-19 and the pharmaceutical environmental pollutant using Materials Studio package. The Heulandite zeolite structure was taken from the package database and its substitutions were carried out according to Lowenstein's and Dempsey's rules to create Clinoptilolite unit cell. The simulations are performed in the constant-volume constant-temperature (NVT) ensemble. Respectively, adsorption energy values of -83.99 and -68.33 kcal/mol were obtained for the Heulandite and Clinoptilolite-based structures following the adsorption of the initial drug. These values indicate that obtained compounds are suitable adsorbents for removing unwanted Favipiravir drug emitted in the environment. To illustrate the diffusion of the drug within the framework structure, mean-squared displacement (MSD) calculations were utilized, revealing that Favipiravir had a greater propensity to diffuse through the Heulandite pore network in comparison to Clinoptilolite.

Keywords: Molecular dynamics simulation, Heulandite, Clinoptilolite, Favipiravir, Adsorption energy, Diffusion.

Introduction

The pandemic caused by the novel coronavirus SARS-CoV-2, a member of the coronavirus family, had created a global health crisis for our planet. Over the past 3 years, COVID-19 infections had become increasingly prevalent, with symptoms such as high fever, cough, myalgia, weakness, and polypnea, often leading to severe respiratory problems and even acute respiratory distress syndrome (ARDS) and death [1,2]. The risk of serious symptoms and mortality is particularly high for individuals over the age of 60 and those with pre-existing medical conditions such as heart, lung, kidney, and liver disease, diabetes, and severe obesity. In response to the pandemic, researchers and medical professionals have been tirelessly working to develop effective treatments, including repurposed and new drugs, interferon-based therapies, and cell and plasma-based treatments. Despite significant efforts to control the spread of the disease and the development of various drugs and vaccines to treat and prevent the virus, a large number of people around the world continue to be infected with different strains of the virus and even lose their lives as a result [3,4]. A wide range of different drugs such as Favipiravir, Remdesivir, Darunavir, Oseltamivir, Umifenovir, Teicoplanin, Azithromycin, Chloroquine, and Hydroxychloroquine, etc. have been applied to treat this infection which some proved beneficial while others were not effective [5-12]. In 2014, Japan introduced Favipiravir, an anti-RNA virus medication, for the treatment of novel or re-emerging influenza viruses. Upon entering the cell, Favipiravir undergoes ribosylation and phosphorylation, which activates and allows it to substitute with purine nucleosides in the virus RNA. As a result, the RNA-dependent RNA polymerase (RdRp) of the virus is inhibited, preventing RNA strand elongation and viral proliferation. Favipiravir has been found to be effective against a broad range of RNA viruses, including

Rhinovirus, Arenavirus, Bunyavirus, Flavivirus, Filovirus causing hemorrhagic fever, as well as the Ebola virus. Notably, the RNA structure of SARS-CoV-2 and its similarity to SARS-CoV have led to Favipiravir being considered a potential treatment candidate for COVID-19 [13] but, some clinical considerations show that the Favipiravir group cardiopulmonary caused, cerebral infarction, liver disorder, and COVID-19-related pneumonia. In addition, Favipiravir similar to other various antiviral drugs is not fully metabolized by the body and is excreted through feces and urine, entering the wastewater system as parent or metabolite compounds. However, the low biodegradability of many antiviral drugs poses a challenge for conventional wastewater treatment systems, that have limited capacity to remove them [14-16]. As a result, significant quantities of antiviral drug residues are discharged into environmental waters. Previous research has demonstrated that these residues found in wastewater can be highly toxic to aquatic organisms such as algae, daphnia, and fish [17, 18].

Zeolites with pore sizes under 2 nm are considered as one of the most important drug carriers and adsorbents. These three-dimensional crystalline aluminosilicates consist of Si and/or Al tetrahedral linked by shared oxygen atoms, creating vast networks of interconnected channels that result in higher internal surface areas. Due to these unique properties, zeolites have become essential in various applications, including catalysis, ion exchange, adsorption, veterinary medicine, zoo technology, tissue engineering, and drug delivery [19-24]. Zeolitic materials also exhibit both thermal and chemical stability and possess well-defined channels and cavities [25, 26]. Naturally occurring zeolites, such as Heulandite and Clinoptilolite, contain extra frameworks cation sites, such as alkali and alkaline-earth cations, which are loosely bound, allowing for rapid exchange with other pollutant cations present in water [27, 28]. These zeolites are commonly described as having monoclinic crystal structures, with space group C2/m, and are classified as HEU-type. The HEU framework comprises three sets of intersecting channels, all located in the (010) plane. The A and B channels, which are parallel to the c-axis, are formed by strongly compressed ten-membered and eight-membered rings, respectively, with apertures of 3.0×7.6 Å and 3.3×4.6 Å. The C channels, which are parallel to the a-axis, are also formed by eight-membered rings, with an aperture of 2.6×4.7 Å. Heulandite is defined as the zeolite mineral with a Si/Al ratio of less than 4.0, while Clinoptilolite, with the same framework topology, has a Si/Al ratio equal to or greater than 4.0. Theoretical and experimental literature reviews demonstration that the use of zeolites as an inexpensive, non-toxic, and targeted framework is highly effective for drug delivery. Lam et al studied Metronidazole adsorption on Clinoptilolite using AM1 semi-empirical method and understood that the interaction is stronger in the 8-ring window than 10-ring window [29]. Lam et al in another research investigated the physical adsorption of Aspirin on Clinoptilolite by applying AM1 and PM3 methods. All values obtained for the adsorption enthalpies were negative, which could explain the adsorption process [30]. Rivera and his coworker explored Clinoptilolite-surfactant composites as drug support experimentally. The drug adsorption assays showed that only the purified natural Clinoptilolite-benzalkonium chloride composite adsorbs a considerable amount of drug, in particular sulfamethoxazole, which was evaluated by UV spectroscopy [31]. Jordanoski et al considered a heulandite-calcium-based as a novel silica-based hemoglobin carrier system. These Particles exhibit superior properties compared to traditional TEOS nanoparticles. In all of these works the Si/Al ratio is approximately 5 and the results suggest that there is a significant potential for their use in the development of biomedical hemoglobin loading and delivery systems [32]. As has been proven, computational studies can give us useful information along with experimental studies. So, in this study, molecular dynamics simulations study was applied to confirm and enhance the understanding of how the drug interacts with Heulandite and Clinoptilolite zeolites.

Molecular Modeling and Simulation Method

Molecular dynamics simulation has been applied to study Favipiravir drug adsorption behavior on Heulandite and Clinoptilolite zeolites at the atomic level. The Heulandite zeolite structure was taken from the Materials Studio package database [33], and its unit cell was created by transforming the asymmetric unit into P1 symmetry while Favipiravir molecular structure was obtained from PubChem (CID: 492405). The placement of aluminum atoms, sodium, and calcium cations was a matter of question in creating the Clinoptilolite structure (Si/Al =5). To address this issue, we utilized the aluminum sites identified in previous theoretical studies [34, 35] that accurately reproduced the experimentally observed partial occupancy. The selected Si atoms in the Heulandite framework were replaced with Al atoms by considering the energy of the system. The substitutions were carried out according to Lowenstein's and Dempsey's rules, where the former prevents the Al–O–Al bridges, which is energetically unflavored and the latter emphasizes on the homogeneity of Al atoms substituted with Si atoms. Therefore, the Si atoms to be replaced were selected so that the resulting frameworks had the minimum energy. In the next step to make the zeolites unit cell complete, 24 water molecules have been added to the structure using the Amorphous Cell module, the Packing task, to soak

structures with a solvent at specified density. Comparing previous studied forcefileds (FF) based on empirical interatomic potentials, it is confirmed that COMPASS (**C**ondensed-phase **O**ptimized **M**olecular **P**otentials for **A**tomistic **S**imulation **S**tudies) has been the best FF for describing all atoms of the zeolites and organic molecules [36]. It uses a hybrid approach in deriving parameter values, with valence parameters fitted to ab initio data, and van der Waals parameters to experimental data [37]. Refinements were made in subsequent generations to the COMPASS forcefield, resulting in the development of the more sophisticated COMPASS III forcefield, and as a result, for this paper, the latest version of this forcefield was chosen. The study utilized nonbonding interactions, including van der Waals atom-based and Coulombic electrostatic interactions and the Ewald summation method. These conditions have been employed previously with successful outcomes [38]. The forcefield was used to calculate atomic charges, ensuring that the zeolite system remained neutral throughout the simulation. In the following, periodic boundary conditions were applied to the crystal lattice structures.

Before conducting the MD simulations, all investigated systems underwent energy minimization and eliminate unfavorable interactions as well as achieve the lowest energy state, geometry optimization was carried out using the smart algorithm; which is a cascade of methods applying successively Steepest descent and Conjugate gradient algorithms of Forcite module in Materials Studio package [33]. Forcite code is an advanced classical molecular mechanics tool, that allows fast energy calculations and reliable geometry optimization of molecules and periodic systems within the Materials Studio package. Optimization was performed on ten structures for each component, and the one with the lowest energy was selected for further investigations.

Following the optimization process, the drug was allowed to freely choose its preferred position for adsorption inside or outside each zeolite pore structure using the adsorption locator module which finds low-energy adsorption sites for structures on both periodic and non-periodic substrates. The obtained energies of the models were used to calculate the adsorption energy (E_{ads}) and their percentage change (ΔE_{ads}) using the following equations (1) and (2), where E_{ads} is the energy of the drug-zeolite adsorption complex, $E_{zeolite}$ and E_{drug} are the energy of zeolite and drug. $E_{ads\,(1)}$ and $E_{ads\,(2)}$ are related to primary and secondary modes of drug-zeolite complexes after the adsorption of (n) and (n+1) drug molecules respectively.

$$E_{ads} = E_{zeolite/drug} - (E_{zeolite} + E_{drug}) \quad (1)$$

$$\Delta E_{ads} = ((E_{ads\,(2)} - E_{ads\,(1)}) / E_{ads\,(1)}) \times 100 \quad (2)$$

In the next step, MD simulations were performed using the NVT ensemble at 310.15 K with the COMPASS III forcefield, applying 1.0 fs time step and Nosé–Hoover thermostat. To assess the movement of Favipiravir, including diffusion within the zeolite pore structure during the simulation, the mean-squared displacement (MSD) was determined using the following equation:

$$MSD = |r_i(t) - r_i(0)|^2 \quad (3)$$

Where $r_i(t)$ is the position of molecule i at time t and $r_i(0)$ is an arbitrary starting point.

Results and Discussions

Zeolite Crystal Structure

As mentioned above, after generating the zeolites unit cell, the atomic positions and crystal lattice were fully optimized, allowing for variable volume. The Heulandite unit cell is monoclinic, belonging to the C2/m space group with lattice parameters of a = 17.76, b = 17.95, c = 7.40Å, and β angle of 116.40°.

The Clinoptilolite unit cell with a molecular formula of $Na_2Ca_2Al_6Si_{30}O_{72}(H_2O)_{24}$ is monoclinic, belongs to the C2/m space group with lattice parameters of a = 17.66, b = 17.91, c = 7.43Å, and β angle of 116.4°. Table 1 presents the calculated parameters, as well as the crystallographic data documented in the zeolite structure database [39]. This issue illustrates a significant level of agreement, validating the accuracy of the calculations. Once the zeolites unit cells was optimized, a suitable supercell with dimensions of 1×1×2 was generated, and the resulting structures were re-optimized (can be seen in Fig.1.) using the same method as described earlier.

Table 1. Calculated and experimental cell parameters of the used zeolites.

Zeolite	a (Å)	b (Å)	c(Å)	α (°)	β (°)	γ (°)
Heulandite (calc.)	17.76	17.95	7.40	90.00	116.40	90.00
Heulandite (exp.)	17.52	17.64	7.40	90.00	116.10	90.00
Clinoptilolite (calc.)	17.66	17.91	7.43	90.00	116.40	90.00
Clinoptilolite (exp.)	17.66	17.91	7.40	90.00	116.40	90.00

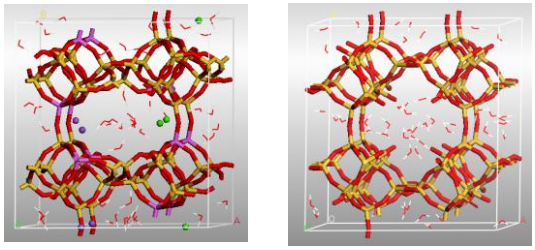

(a) **(b)**

Fig.1. Optimized crystal structures of (a) Heulandite and (b) Clinoptilolite 1×1×2 supercells. The Si, O, H, Al, Na, and Ca atoms are represented in yellow, red, white, pink, purple and green colors, respectively.

Through the process of optimization calculation, the most stable structure of the Favipiravir model with $C_5H_4FN_3O_2$ molecular formula was determined, possessing a size of 7.70×6.60 Å. The molecule has a three-dimensional structure due to the presence of multiple functional groups attached to the pyrazine ring that you can see its simple flat structure in Fig.2. The pyrazine ring itself is planar, but the carboxyl, amide, and hydroxyl groups attached to it cause the molecule to adopt a non-planar conformation which helps to introduce it to supercell of zeolite. In addition, the literature review shows that Favipiravir is known to have several enol-like and keto-like tautomer whose relative stability depends on the environment of oxygen groups which is in the presence of water; a keto form appears to be favored. According to the theoretical simulations, the metal ion is captured between the carbonyl groups as a result of the size–fit effect [40, 41]. Also, the actual conformation of the molecule can be affected by its environment, such as intermolecular interactions or crystal packing. Therefore, in the case of natural zeolite the presence of water and alkaline earth in the cages, the keto form of Favipiravir is considered. Additionally, Molecular electrostatic potential (MEP) analysis was carried out to study the interaction between the drug and zeolites. The MEP plot illustrates electrostatic potential mapped onto the total electron density surface. This graph provides information about the correlation between molecular structure with its physiochemical properties including partial charges, dipole moment, and chemical reactivity. It shows the locations of the various most positive and most negative regions in which the blue area, refers to the regions of positive potential (hydrogen atoms) and corresponds to electron-poor regions; whereas the red color signifies the negative potential (oxygen and fluorine atoms) and related to electron-rich areas. Fig.2. displays the bond lengths of the Favipiravir molecule as well as the MEP surface after the completion of geometry optimization.

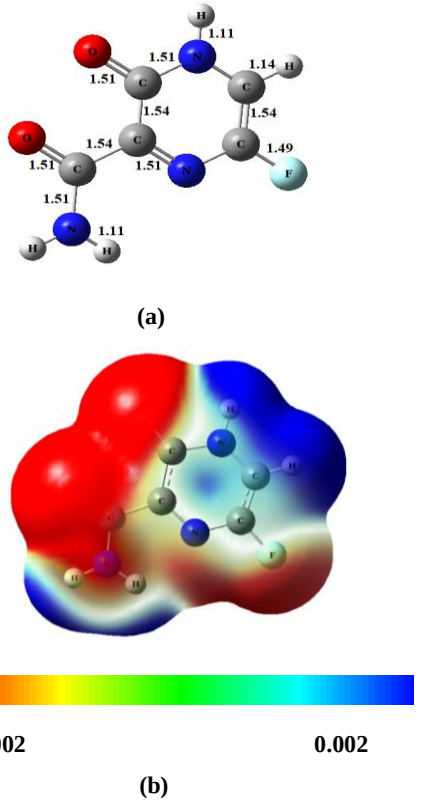

(a)

(b)

Fig.2. (a) Optimized molecular structure, and (b) MEP surface of Favipiravir drug (The surfaces are defined by the 0.002 electrons/b 3 contour of the electronic density. Color ranges, in a.u.)

Adsorption of Favipiravir in Zeolites

After modeling of zeolites structure, adding water molecules, and optimizing zeolites as well as drug molecule, in contrast to the majority of studies that involve placing a drug molecule manually into a zeolite cavity; we employed adsorption locator module to allow the drug molecule to remain unbound, enabling it to be positioned randomly either inside or outside the zeolite cavity. So, the mentioned module was applied 5 times to check the effect of 1-5 drugs to determine their impact and location within the target system. Then, the formed complexes were re-optimized to calculate the adsorption energy values, providing insight into the energy required for drug adsorption into the system. It should be mentioned that the zeolite structures crystalline parameters remained steady. The final position of Favipiravir drug adsorbed in Heulandite and Clinoptilolite zeolite structures can be seen in Fig 3 and 4 respectively. The first, fourth, and fifth drug molecules tended to adsorb onto the surface, while the second and third molecules penetrated the zeolite channel. It is noteworthy that for Clinoptilolite, only the third drug molecule was able to penetrate the zeolite channel, this reduction in drug penetration compared to Heulandite is due to the presence

of sodium and calcium cations in the Clinoptilolite structure, which has led to a decrease in accessible free space.

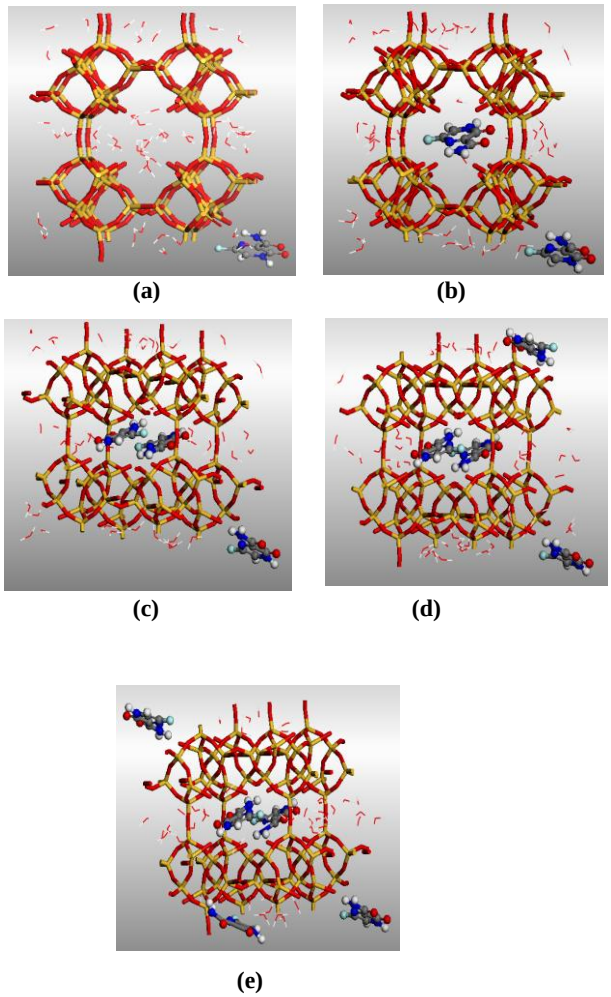

Fig. 3. Optimized adsorption complexes of Heulandite include one, two, three, four, and five Favipiravir molecules as (a), (b), (c), (d), and (e) respectively.

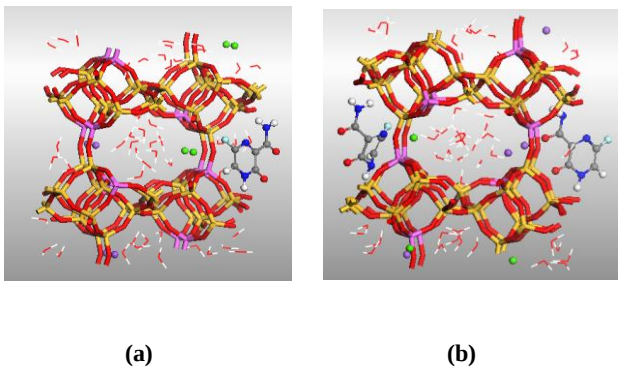

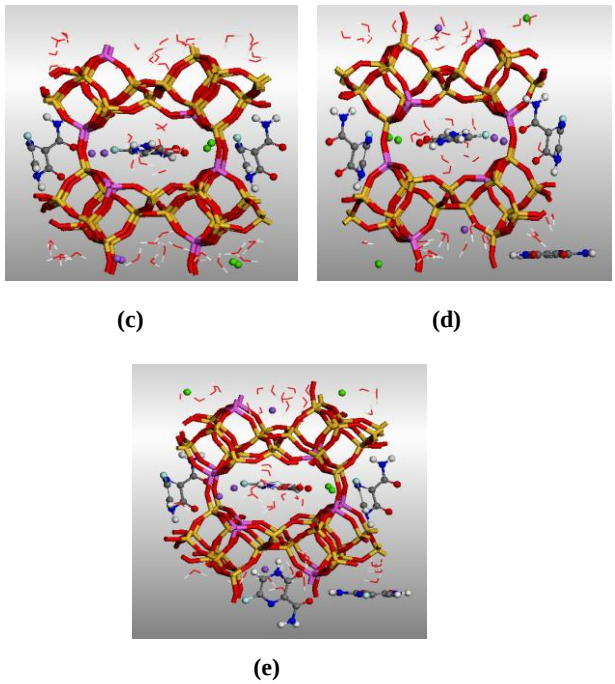

Fig. 4. Optimized adsorption complexes of Clinoptilolite includes one, two, three, four, and five Favipiravir molecules as (a), (b), (c), (d), and (e) respectively.

The subsequent step involved calculating the adsorption energy values (E_{ads}), and their percentage change (ΔE_{ads}) for all the complexes obtained using Equation (1) and (2) respectively which are presented in Table 2. Since all the adsorption energy values are negative, we can conclude that obtained structures are thermodynamically favorable and both zeolites could be potential adsorbents for Favipiravir. It is important to note that very high energy values are not ideal for drug delivery systems as they can impede drug release and create complications while it can lead to the formation of an effective chemical bond occurring in applications aimed at removing harmful substances from our environment. Interestingly, the surface of both zeolites was the preferred adsorption site for the initially loaded drugs, rather than the pores. The adsorption energy values, which were -83.99 and -68.33 kcal/mol for Heulandite and Clinoptilolite zeolites respectively, suggest that the simpler framework of Heulandite facilitated easier adsorption and the creation of a more stable structure for the drug molecule. Given that the adsorption energy of the third drug molecule that penetrated the Clinoptilolite cavity (-202.83 kcal/mol) is nearly equal to that of the second drug molecule that entered the Heulandite pore (-227.78 kcal/mol), it appears that Heulandite has greater adsorption capacity under comparable conditions. On the other hand, the amount of adsorption energy percentage change (ΔE_{ads}) from the first to the second drug molecule in Heulandite and

Clinoptilolite zeolites has reached 83.65% to 11% as well as 83.81% to 15.57% in molecules 4 to 5, respectively. These results suggest a reduced propensity to absorb additional drugs, which can be potentially indicated the onset of saturation. For a better understanding of adsorption energies, some nanostructure adsorbents tendency toward Favipiravir adsorbing using quantum mechanical methods (Density Functional Theory: DFT) has been mentioned in the gas phase and water media in Table. 3. Except of SiC_{19}, all other structures exhibit an adsorption energy of less than 30kcal/mol which this level of adsorption can be made these structures suitable candidates for drug carriers. Indeed, given the appropriate conditions, they can keep the drug properly and then release it at the desired locations. Moreover, as it is clear in Figures 3 and 4, in the situations where Favipiravir showed a tendency to surface adsorption, it approached the zeolite surface from the side of oxygen or fluorine atoms (rich in electrons). Molecular electrostatic potential suggests that the Favipiravir molecule is more positive compared to Heulandite and Clinoptilolite confirming a charge transfer from the drug molecule to the surface of zeolites.

Table 2. Adsorption energies (E_{ads}), their percentage change (ΔE_{ads}) of complexes generated with Heulandite/Clinoptilolite and Favipiravir (Fvr) as well as the drug location.

Complex	Supercell	Number of drug molecules	E_{ads} (kcal/mol)	ΔE_{ads} (%)	Drug location (after adsorption)
Heulandite-1Fvr	1×1×2	1	-83.99	-	On the surface
Heulandite-2Fvr	1×1×2	2	-154.25	83.65	**Inside the pore**
Heulandite-3Fvr	1×1×2	3	-227.78	47.67	**Inside the pore**
Heulandite-4Fvr	1×1×2	4	-301.39	32.32	On the surface
Heulandite-5Fvr	1×1×2	5	-334.56	11.00	On the surface
Clinoptilolite -1Fvr	1×1×2	1	-68.33	-	On the surface
Clinoptilolite -2Fvr	1×1×2	2	-125.60	83.81	On the surface
Clinoptilolite -3Fvr	1×1×2	3	-202.83	61.49	**Inside the pore**
Clinoptilolite -4Fvr	1×1×2	4	-323.52	59.50	On the surface
Clinoptilolite -5Fvr	1×1×2	5	-373.88	15.57	On the surface

Table 3. Theoretical adsorption energies of Favipiravir onto some other absorbents in gas phase and water media.

Adsorbents	Computational Method and basis set	E_{ads} (kcal/mol) in gas phase	E_{ads} (kcal/mol) in water media
Graphene [42]	PBE/ 6-311+G (2d, p)	-14.23	-17.61
BC3 [42]	PBE/ 6-311+G (2d, p)	-23.67	-27.08
NC3 [42]	PBE/ 6-311+G (2d, p)	-18.51	-21.78
$B_{12}N_{12}$ [43]	WB97XD/ 6-31G (d, p)	-20.44	-22.70
SiC_{19} [44]	M062X/ 6-31G (d, p)	-43.46	-51.24

MSD Results

To have a deeper understanding of zeolites behavior in drug adsorption process, we investigated the MSD analysis in this section. Fig.5. displays the profiles of MSD versus time for the drug confined in the pore structure of each zeolite, which was obtained at a temperature of 310.15 K. The Heulandite cavity's larger size, resulting from the absence of cations, allows for easier drug penetration compared to Clinoptilolite. Additionally, the graph in this section depicts the slope of drug penetration is relatively steeper in Heulandite than in Clinoptilolite, which aligns with previous findings.

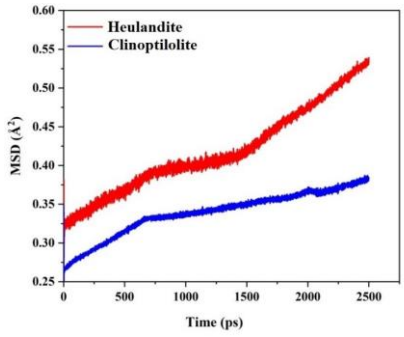

Fig. 5. MSD vs. time graphs for Favipiravir diffusion through Heulandite and Clinoptilolite framework.

Conclusions

During the coronavirus epidemic, Favipiravir was identified as a potentially effective treatment if administered in the correct dosage, even though it may have biodegradability effects. In contrast to the majority of studies that aim to identify a suitable carrier for drugs like this one, our focus in the present study was on developing an environmentally friendly and safe adsorbent that could effectively gather and adsorb excess amounts of the drug from the surrounding environment, without posing a risk to human health. For this purpose, molecular dynamics simulations via the Materials Studio package have been performed to compare two HEU family zeolites adsorption abilities. The results indicate that both Heulandite and Clinoptilolite have significant potential as safe adsorbents, with Heulandite being the more suitable candidate.

References

[1]. Gorbalenya, A. E., Baker, S. C. R., Baric, S. R., de Groot, J., Drosten, C., Gulyaeva, A. A., Haagmans, B., Lauber, C., Leontovich, A. M., Neuman, B. W., Penzar, D., Perlman, S., Poon, L. L. M., Samborskiy, D. V., Sidorov, I. A., Sola, I., Ziebuhr. J., The species Severe acute respiratory syndrome-related coronavirus: classifying 2019-nCoV and naming it SARS-CoV-2, ***Nature microbiology***, ***2020***, *5(4)*, 536.
https://doi.org/10.1038/s41564-020-0695-z.

[2]. Aytür,Y. K., Köseoğlu, B. F., Taşkıran, Ö. Ö., Ordu-Gökkaya, N. K., Delialioğlu, S. Ü., Tur, B. S., Sarıkaya, S., Şirzai, H., Tiftik, T. T., Alemdaroğlu, E., Ayhan, F. F., Pulmonary rehabilitation principles in SARS-COV-2 infection (COVID-19): A guideline for the acute and subacute rehabilitation, ***Turkish Journal of Physical Medicine and Rehabilitation***, **2020**, 66(2), 104. https://doi.org10.5606/tftrd.2020.6444.

[3]. Wang, L., He, W., Yu, X., Hu, D., Bao, M., Liu, H., ... & Jiang, H., Coronavirus disease 2019 in elderly patients: characteristics and prognostic factors based on 4-week follow-up, ***Journal of Infection***, **2020**, *80*(6), 639. https://doi.org/10.1016/j.jinf.2020.03.019.

[4]. Skariyachan, S., Gopal, D., Chakrabarti, S., Kempanna, P., Uttarkar, A., Muddebihalkar, A. G., & Niranjan, V., Structural and molecular basis of the interaction mechanism of selected drugs towards multiple targets of SARS-CoV-2 by molecular docking and dynamic simulation studies-deciphering the scope of repurposed drugs. ***Computers in Biology and Medicine***, **2020**, *126*, 104054.
https://doi.org/10.1016/j.compbiomed.2020.104054.

[5]. Tarighi, Parastoo, Samane Eftekhari, Milad Chizari, Mahsa Sabernavaei, Davod Jafari, and Parastoo Mirzabeigi. "A review of potential suggested drugs for coronavirus disease (COVID-19) treatment, ***European Journal of Pharmacology***, **2021**, 895,173890.
https://doi.org/10.1016/j.ejphar.2021.173890.

[6]. Yadav, P., Rana, M., & Chowdhury, P., DFT and MD simulation investigation of favipiravir as an emerging antiviral option against viral protease (3CLpro) of SARS-CoV-2, ***Journal of Molecular Structure***, **2021**, *1246*, 131253.
https://doi.org/10.1016/j.molstruc.2021.131253.

[7]. Khanal, P., Remdesivir for COVID-19 treatment: mechanism OF action, synthesis, and clinical trials, ***Journal of Pharmacy and Pharmaceutical Science***, **2020**, *9*(8), 1062.
https://doi.org/10.20959/wjpps20208-16808.

[8]. Beck, B.R., Shin, B., Choi, Y., Park, S. and Kang, K., Predicting commercially available antiviral drugs that may act on the novel coronavirus (SARS-CoV-2) through a drug-target interaction deep learning model, ***Computational and Structural Biotechnology Journal***, **2020**, *18*, 784.
https://doi.org/10.1016/j.csbj.2020.03.025.

[9]. Lian, N., Xie, H., Lin, S., Huang, J., Zhao, J., & Lin, Q., Umifenovir treatment is not associated with improved outcomes in patients with coronavirus disease 2019: a retrospective study. ***Clinical Microbiology and Infection***, **2020**, *26*(7), 917.
https://doi.org/10.1016/j.cmi.2020.04.026.

[10]. Ceccarelli, G., Alessandri, F., d'Ettorre, G., Borrazzo, C., Spagnolello, O., Oliva, A., ... & Venditti, M., Is teicoplanin a complementary treatment option for COVID-19? The question remains, ***International Journal of Antimicrobial Agents***, **2020**, *56*(2), 106029.
https://doi.org/10.1016/j.ijantimicag.2020.106029.

[11]. Furtado, R. H., Berwanger, O., Fonseca, H. A., Corrêa, T. D., Ferraz, L. R., Lapa, M. G., ... & Cavalcanti, A. B., Azithromycin in addition to standard of care versus standard of care alone in the treatment of patients admitted to the hospital with severe COVID-19 in Brazil (COALITION II): a randomised clinical trial, ***The Lancet***, **2020**, *396*(10256), 959.
https://doi.org/10.1016/S0140-6736(20)31862-6.

[12]. Cavalcanti, A. B., Zampieri, F. G., Rosa, R. G., Azevedo, L. C., Veiga, V. C., Avezum, A., ... & Berwanger, O., Hydroxychloroquine with or without Azithromycin in Mild-to-Moderate Covid-19, ***New England Journal of Medicine***, **2020**, *383*(21), 2041.
https://doi.org/10.1056/NEJMoa2019014.

[13]. Shiraki, K., & Daikoku, T., Favipiravir, an anti-influenza drug against life-threatening RNA virus infections, ***Pharmacology & therapeutics***, **2020**, *209*, 107512.
https://doi.org/10.1016/j.pharmthera.2020.107512.

[14]. Nannou, C., Ofrydopoulou, A., Evgenidou, E., Heath, D., Heath, E., & Lambropoulou, D., Antiviral drugs in aquatic environment and wastewater treatment plants: a review on occurrence, fate, removal and

ecotoxicity, ***Science of the Total Environment***, **2020**, *699*, 134322.
https://doi.org/10.1016/j.scitotenv.2019.134322.
[15]. Mlunguza, N. Y., Ncube, S., Mahlambi, P. N., Chimuka, L., & Madikizela, L. M., Determination of selected antiretroviral drugs in wastewater, surface water and aquatic plants using hollow fibre liquid phase microextraction and liquid chromatography-tandem mass spectrometry, ***Journal of Hazardous Materials***, **2020**, *382*,121067
https://doi.org/10.1016/j.jhazmat.2019.121067.
[16]. Zhao, X., Chen, J., Guo, M., Li, C., Hou, N., & Bai, S., Constructed wetlands treating synthetic wastewater in response to day-night alterations: performance and mechanisms, ***Chemical Engineering Journal***, **2022**, *446*, 137460.
https://doi.org/10.1016/j.cej.2022.137460.
[17]. Race, M., A. Ferraro, E. Galdiero, M. Guida, A. Núñez-Delgado, F. Pirozzi, A. Siciliano, and M. Fabbricino. "Current emerging SARS-CoV-2 pandemic: potential direct/indirect negative impacts of virus persistence and related therapeutic drugs on the aquatic compartments, ***Environmental Research***, ***2020***, 188, 109808. https://doi.org/10.1016/j.envres.2020.109808.
[18]. Sanderson, H., Johnson, D. J., Reitsma, T., Brain, R. A., Wilson, C. J., & Solomon, K. R., Ranking and prioritization of environmental risks of pharmaceuticals in surface waters, ***Regulatory Toxicology and Pharmacology***, **2004**, *39*(2), 158.
https://doi.org/10.1016/j.yrtph.2003.12.006.
[19]. A. J. Schwanke, R. Balzer, S. Pergher, L. M.T. Martínez, O. V. Kharissova, B. I. Kharisov, *Handbook of Ecomaterials*, 2017, 1–22 .
[20]. Bacakova, L., Vandrovcova, M., Kopova, I., & Jirka, I., Applications of zeolites in biotechnology and medicine–a review, ***Biomaterials Science***, **2018**, *6*(5), 974.
https://doi.org/10.1039/C8BM00028J.
[21]. Karavasili, C., Kontogiannidou, E., Chatzitaki, A. T., Barmpalexis, P., & Fatouros, D. G., Experimental and molecular dynamics simulation studies of an anti-hyperlipidemic drug release from microporous zeolites differing in Si/Al content, ***Microporous and Mesoporous Materials***, **2020**, *305*, 110343.
https://doi.org/10.1016/j.micromeso.2020.110343.
[22]. Souza, I.M., Sainz-Díaz, C.I., Viseras, C. and Pergher, S.B., Adsorption capacity evaluation of zeolites as carrier of isoniazid, ***Microporous and Mesoporous Materials***, **2020**, *292*, 109733.
https://doi.org/10.1016/j.micromeso.2019.109733.
[23]. Souza, I.M., Borrego-Sánchez, A., Rigoti, E., Sainz-Díaz, C.I., Viseras, C. and Pergher, S.B., Experimental and molecular modelling study of beta zeolite as drug delivery system, ***Microporous and Mesoporous Materials***, **2021**, *321*, 111152.
https://doi.org/10.1016/j.micromeso.2021.111152.
[24]. Souza, I.M., Borrego-Sánchez, A., Sainz-Díaz, C.I., Viseras, C. and Pergher, S.B., Study of Faujasite zeolite as a modified delivery carrier for isoniazid, ***Materials Science and Engineering: C***, **2021**, *118*, 111365.
https://doi.org/10.1016/j.msec.2020.111365.
[25]. Mortier, W.J. and Schoonheydt, R.A., Surface and solid state chemistry of zeolites, ***Progress in Solid State Chemistry***, **1985**, *16*(1-2), 1.
https://doi.org/10.1016/0079-6786(85)90002-0.
[26]. Lopes, A.C., Martins, P. and Lanceros-Mendez, S., Aluminosilicate and aluminosilicate based polymer composites: present status, applications and future trends, ***Progress in Surface Science***, **2014**, *89*(3-4), 239.
https://doi.org/10.1016/j.progsurf.2014.08.002.
[27]. Alberti. A., The Crystal Structure of Two Clinoptilolites, ***Tschermask Mineralogische und Petrographische Mitteilungen***, **1975**, 22, 25.
[28]. Koyama, K. and Takeuchi, Y., Clinoptilolite: the distribution of potassium atoms and its role in thermal stability, ***Zeitschrift für Kristallographie-Crystalline Materials***, **1977**, *145*(1-6), 216.
[29]. Lam, A., Rivera, A. and Rodrídguez-Fuentes, G., Theoretical study of metronidazole adsorption on clinoptilolite, ***Microporous and Mesoporous Materials***, **2001**, *49*(1-3), 157.
https://doi.org/10.1016/S1387-1811(01)00413-9.
[30]. Lam, A., Sierra, L.R., Rojas, G., Rivera, A., Rodrıguez-Fuentes, G. and Montero, L.A., Theoeretical study of the physical adsorption of aspirin on natural clinoptilolite, ***Microporous and Mesoporous Materials***, **1998**, *23*(5-6), 247. https://doi.org/10.1016/S1387-1811(98)00060-2.
[31]. Rivera, A. and Farias, T., Clinoptilolite–surfactant composites as drug support: A new potential application, ***Microporous and Mesoporous Materials***, **2005**, *80*(1-3), 337.
https://doi.org/10.1016/j.micromeso.2005.01.011.
[32]. Jordanoski, D., Drobne, D., Repar, N., Dogsa, I., Mrak, P., Cerc-Korošec, R., Škapin, A.S., Nadrah, P. and Poklar Ulrih, N., A Novel Artificial Hemoglobin Carrier Based on Heulandite-Calcium Mesoporous Aluminosilicate Particles, ***International Journal of Molecular Sciences***, **2022**, *23*(13), 7460.
https://doi.org/10.3390/ijms23137460.
[33]. BIOVIA, Dassault Systèmes BIOVIA, Materials Studio, 2020, (20.1.02728).
[34]. Ruiz-Salvador, A. R., Gómez, A., Lewis, D. W., Catlow, C. R. A., Rodríguez-Albelo, L. M., Montero, L. and Rodríguez-Fuentes, G., Clinoptilolite–heulandite polymorphism: structural features from computer simulation, ***Physical Chemistry Chemical Physics***, **2000**, *2*(8), 1803.
https://doi.org/10.1039/A909671J.
[35]. Abatal, M., Ruiz-Salvador, A. R., & Hernández, N. C., A DFT-based simulated annealing method for the optimization of global energy in zeolite framework

systems: Application to natrolite, chabazite and clinoptilolite, ***Microporous and Mesoporous Materials***, **2020**, *294*, 109885. https://doi.org/10.1016/j.micromeso.2019.109885.
[36]. Sun, H., COMPASS: an ab initio forcefield optimized for condensed-phase applications overview with details on alkane and benzene compounds, ***The Journal of Physical Chemistry B***, **1998**, *102*(38), 7338.
[37]. Escamilla-Roa, E., Huertas, F. J., Hernández-Laguna, A. and Sainz-Díaz, C. I., A DFT study of the adsorption of glycine in the interlayer space of montmorillonite, ***Physical Chemistry Chemical Physics***, **2017**, *19*(23), 14961. https://doi.org/10.1039/C7CP02300F.
[38]. Sainz-Díaz, C. I., Francisco-Márquez, M. and Vivier-Bunge, A., Adsorption of polyaromatic heterocycles on pyrophyllite surface by means of different theoretical approaches, ***Environmental Chemistry***, **2011**, *8*(4), 429. https://doi.org/10.1071/EN11055.
[39]. C. Baerlocher, L. B. McCusker, Database of zeolite structures, http://www.iza-structure.org/ databases/, 2017.
[40]. L. Antonov, http://www.tautomer.eu, 2020.
[41]. Deneva, V., Slavova, S., Kumanova, A., Vassilev, N., Nedeltcheva-Antonova, D. and Antonov, L., Favipiravir—tautomeric and complexation properties in solution, ***Pharmaceuticals***, **2022**, *16*(1), 45. https://doi.org/10.3390/ph16010045.
[42]. Al-Qargholi, B., Tabassum, S., Abbass, R., Al-Saidi, D. N., Gatea, M. A., Fazaa, A. H., Saraswat, S. K., Petrosian, S. and Li, W., Nanosheets (CC-BC_3-C_3N) as an carrier for favipiravir drug: A density functional theory study, ***Inorganic Chemistry Communications***, **2023**,*150*, 110475. https://doi.org/10.1016/j.inoche.2023.110475.
[43]. Hasan, M. M., Das, A. C., Hossain, M. R., Hossain, M.K., Hossain, M.A., Neher, B. and Ahmed, F., The computational quantum mechanical investigation of the functionalized boron nitride nanocage as the smart carriers for favipiravir drug delivery: a DFT and QTAIM analysis, ***Journal of Biomolecular Structure and Dynamics***, **2022**, *40*(23), 13190. https://doi.org/10.1080/07391102.2021.1982776.
[44]. Alver, Ö., Parlak, C., Umar, Y. and Ramasami, P., DFT/QTAIM analysis of favipiravir adsorption on pristine and silicon doped C_{20} fullerenes, ***Main Group Metal Chemistry***, **2019**, *42*(1), 143. https://doi.org/10.1515/mgmc-2019-0016.